

# Osteoconductivity Evaluation of 3-Dimensional Dual-leached Polycaprolactone Scaffold

Pratchayaporn Aksorn<sup>1</sup>, Daneeya Chaikiawkeaw<sup>2</sup>, Panunn Sastravaha<sup>1</sup>, Pitt Supaphol<sup>3</sup>, Prasit Pavasant<sup>2</sup>

<sup>1</sup>Department of Oral and Maxillofacial Surgery, Faculty of Dentistry, Chulalongkorn University, Bangkok, Thailand

<sup>2</sup>The Center of Excellence in Regenerative Dentistry (CERD), Faculty of Dentistry, Chulalongkorn University, Bangkok, Thailand

<sup>3</sup>The Petroleum and Petrochemical College, Chulalongkorn University, Bangkok, Thailand

## Abstract

Recently, the dual-leached polycaprolactone (DL-PCL) scaffold for bone tissue engineering had been fabricated using sodium salt and polyethylene glycol as porogens. This novel scaffold showed good porous inter-connectivity and did not have any cytotoxicity as judged by SEM analysis and MTT assay. The purpose of this study was to evaluate the *in vitro* biocompatibility and osteogenic conductive potential of this DL-PCL scaffold on the bone formation *in vivo*. Periodontal ligament stem cells were seeded on the DL-PCL scaffold for 16 hours and the morphology of cells on the scaffold was assessed by SEM analysis. The expression of osteogenic related genes was also determined by real-time reverse transcription polymerase chain reaction (RT-PCR). The ability of the DL-PCL scaffold to support new bone formation was examined in a rat calvarial defect model. The total IgG from blood serum was measured after scaffold implantation at two, four and eight weeks. The amount and quality of new bone formation were monitored by micro-computed tomography and histological analysis, respectively. The results showed that periodontal ligament stem cells attached and spread on the DL-PCL scaffold and expressed the markers of osteogenic differentiation including ALP, RUNX2 and OSX. There were no significant changes in the level of serum IgG after the scaffolds were implanted. Micro-computed tomography and histological analysis in a rat calvarial model showed a significantly greater amount of new bone formation. These results indicated the ability of DL-PCL for the use of bone tissue engineering.

**Keywords:** Bone tissue engineering, Calvarial defect, Dual-leaching scaffold, Polycaprolactone, Solvent casting/Particulate leaching method, Three-dimensional porous scaffold

**Grants:** This study was supported by the 2012 Research Chair Grant from the National Science and Technology Development Agency (NSTDA). The Center of Excellence for Regenerative Dentistry was supported by the Chulalongkorn Academic Advancement into Its 2<sup>nd</sup> Century Project.

Received date:

Revised date:

Accepted date:

Doi:

Correspondence to :

Prasit Pavasant, Center of Excellence in Regenerative Dentistry (CERD), Faculty of Dentistry, Chulalongkorn University, Henri-Dunant Road, Wangmai, Pathumwan, Bangkok 10330 Thailand. E-mail: prasit.pav@chula.ac.th

## Introduction

Large bone defects resulting from tumor resection, trauma, non-union of fractures, and congenital malformations are common clinical problems in maxillofacial surgery. Several methods have been used for bone reconstruction in the maxillofacial region to solve the previously mentioned problems, which include autogenous bone grafts, allografts, alloplasts and xenografts.<sup>1,2</sup> Autogenous bone graft has been the gold standard of bone replacement for many years because it provides osteogenic cells as well as essential osteoinductive factors needed for bone healing and regeneration. However, this practice is limited by donor-site morbidity and the limited amount of bone that can be obtained. These limitations have inspired a search for innovative techniques for bone bioengineering and developing more suitable biomaterials.<sup>3-5</sup>

The concept of tissue engineering can be defined as the use of a combination of cells, engineering material or scaffold to support the growth and differentiation of cells and the proper biochemical factors to improve or replace biological functions.<sup>6,7</sup> The main principle for bone tissue engineering strategy is to use an osteoconductive porous scaffold in combination with osteogenic cells or osteoinductive biochemical factors that can improve or replace the biological function of the bone.<sup>6-8</sup> The scaffold is the first requirement needed to facilitate the tissue integration into the bone defect; a three-dimensional (3D) porous scaffold will function as a template for cell attachment, proliferation and differentiation of bone cells.<sup>9-11</sup>

Several natural and synthetic polymers have been used to fabricate tissue engineering scaffolds. Aliphatic polyesters such as polycaprolactone (PCL), polylactic acid (PLA), polyglycolic acid and related copolymers are most extensively used in biodegradable scaffolds. PCL is a semicrystalline polyester that is degraded by the hydrolysis of its ester linkages under physiological conditions, such as in the human body. This polymer has received FDA approval and is currently used in clinical practice. Its excellent mechanical, slow biodegradation rate and biocompatibility characteristics were previously highlighted. Moreover, it

is significantly less expensive, readily available in large quantities and can be molded into porous structures to allow for osteoconduction.<sup>12,13</sup>

During the past year, many techniques have been applied for making porous scaffolds. These include solvent casting combined with particulate leaching, freeze drying, electrospinning, phase separation, melt molding, and combinations of these techniques. Solvent casting combined with particulate leaching is a technique that results in highly porous structures.<sup>10</sup>

In our previous research<sup>14</sup>, a three dimensional PCL scaffold was fabricated using a modified solvent casting, particulate leaching. By using both sodium chloride and polyethylene glycol (PEG) powders as porogens, a newly synthesized dual-leached (DL) PCL scaffold has been fabricated. The *in vitro* analysis reported that this DL-PCL scaffold exhibited highly interconnected pore networks, equally distributed pores, and a relatively uniform pore size of 378–435  $\mu\text{m}$ , further leading to high water absorption capacity of the materials tested. An indirect cytotoxicity evaluation using mouse calvaria-derived preosteoblastic cells (MC3T3-E1) revealed that the scaffolds were not harmful to the cells. The cells cultured on DL-PCL scaffolds also yielded better mineral deposition values compared to the original PCL scaffold. However, the effectiveness of this scaffold to promote new bone formation is still unclear.

The purpose of this work was to evaluate the potential of the DL-PCL scaffold as bone scaffolding material. The scaffold was assessed *in vitro* in terms of the ability of the scaffolds to support the adhesion and differentiation, as judged by the expression of osteogenic related genes by primary human periodontal ligament (PDL) cells. Finally, the scaffolds were assessed *in vivo* based on the calvarial defect model in rats. The interaction between scaffold and immune response was assessed by the serum IgG of rats. Bone regeneration in the calvarial defects was evaluated by micro-computed tomography (micro-CT) and histological analysis four weeks and eight weeks after implantation.

## Materials and Methods

### Materials

PCL (Molecular weight (MV) 80,000 g/mol) was purchased from Sigma-Aldrich (St. Louis, MO), and PEG (MW 200, 600, and 1,000 g/mol) was purchased from Merck (Germany). Chloroform (Labscan Asia, Thailand) was used as a solvent for these polyesters, whereas sodium chloride (NaCl; Ajax Finechem, Australia) was used as a porogen.

### Preparation of 3D DL-PCL scaffolds

The three-dimensional scaffolds were fabricated as previously reported.<sup>14</sup> Briefly, polymer solution was prepared by mixing a PCL pellet with PEG (PCL/PEG = 1/1 (w/w)) and chloroform at a concentration of 28% (w/v). The solution was then stirred at room temperature for two to three hours. Next, NaCl particles ranging in diameter from 400 to 500  $\mu\text{m}$  (polymer/NaCl = 1/30 (w/w)) were added. The mixture was packed into petri dishes, creating cylindrical scaffolds that were 10 cm in diameter and 0.5 mm in thickness. Scaffolds were placed in a ventilation hood overnight to allow for solvent evaporation. After evaporation, the porogens were leached out by immersing the scaffold in deionized (DI) water for 48 hours, with repeated changes of the DI water every eight hours. The scaffolds were then air-dried for 24 hours and vacuum-dried overnight.

### Isolation and culture of the primary human periodontal ligament cells

Human PDL cells were isolated from periodontal ligament tissues obtained from the third molars extracted for orthodontic reasons. The protocol was approved by the Human Ethical Committee from the Faculty of Dentistry, Chulalongkorn University (HREC-DCU-2012-079). All patients gave informed consent. Third molars from three healthy young individuals without systemic and oral infection, age between 18-25 years old, were obtained. The periodontal ligament tissue from the middle one-third was scraped off with a surgical blade. The tissue explants were cultured in Growth Medium [GM; Dulbecco Modified Eagle medium (DMEM) supplemented with 10% FBS, 1% L-Glutamine, 0.5 mg/ml gentamicin and 3 mg/ml amphotericin B] and

grew at 37°C humidified atmosphere with 5% CO<sub>2</sub>. The medium and all the supplements were obtained from Gibco (Life Technologies Corporation, Grand Island, NY). After the outgrowing cells reached confluence, cells were subcultured at the ratio 1:3 and cells at the 3rd–5th passages were used for the experiments.

### Reverse-transcription polymerase chain reaction

Human PDL cells were seeded in 12-well at a density of 100,000 cells/well and grew for two days in either growth medium (GM) or osteogenic media [OM; GM supplemented with ascorbic acid (50 mg/ml) and  $\beta$ -glycerophosphate (10 mM)]. The same density of cells was also seeded in DL-PCL scaffold and cultured in OM medium for two days. The scaffolds were prepared in circular shape (5 mm in diameter and 1 mm thickness). Total cellular RNA was extracted with TRI Reagent (Roche Diagnostics) according to the manufacturer's instructions. The RNA pellet was washed with 70% ethanol, air dried, and reconstituted in RNase free water.

Each RNA sample (1  $\mu\text{g}$ ) was converted to cDNA by avian myeloblastosis virus (AMV) reverse transcriptase (Promega, WI) for 1.5 hours at 42°C. Subsequently, semi-quantitative PCR was performed. Cycling conditions were set at 95°C for 30 seconds followed by 40 cycles of 95°C for three seconds and 60°C for 30 seconds. The amount of PCR product was calculated based on the quantitation cycle and normalization to the expression of glyceraldehyde 3-phosphate dehydrogenase (GAPDH) gene. The primers were prepared following the reported sequences from GenBank. The oligonucleotide sequences of the primers for alkaline phosphatase (ALP: forward 5' CGA GAT ACA AGC ACT CCC ACT TC 3', reverse 5' CTG TTC AGC TCG TAC TGC ATG TC 3'), runt-related transcription factor 2 (RUNX2: forward 5' ATG ATG ACA CTG CCA CCT CTG A 3', reverse 5' GGC TGG ATA GTG CAT TCG TG 3'), osterix (OSX: forward 5' GCC AGA AGC TGT GAA ACC TC 3', and reverse 5' GCT GCA AGC TCT CCA TAA CC 3') and GAPDH (forward 5'-TGA AGG TCG GAG TCA ACG GAT-3'

and reverse 5'-TCA CAC CCA TGA CGA ACA TGG-3'). The real-time PCR was performed in a LightCycler instrument (Roche Diagnostics, USA) using the LightCycler 480SYBR Green-I Master Kit according to the manufacturer's recommendations.

#### **Morphological observation of cultured cells**

Cells were seeded in the DL-PCL scaffold as described above for 16 hours in GM and fixed with 2.5% glutaraldehyde solution (Sigma, USA) for 30 min. The samples were extensively washed with PBS and dehydrated in ethanol solutions of increasing concentration (30, 50, 70, 90, and 100%) for approximately two minutes at each concentration. The specimens were dried in 100% hexamethyldisilazane (HMDS; Sigma, USA) for five minutes and air-dried after removal of the HMDS. Once completely dry, the specimens were mounted on an SEM stub, coated with gold, and observed under SEM (JSM-5200, JEOL model, Tokyo)

#### **Rat calvarial defect model**

The experiment was carried out on six-week-old wistar rats. The protocol was approved by the Animal Care and Use Ethical Committee, Faculty of Medicine, Chulalongkorn University (Animal Use Protocol No. 1773019). Bilateral circular calvarial defects (5 mm in diameter) were created under general anesthesia with xylazine and ketamine intraperitoneal injection. A total of ten rats were used and divided into two groups; for the DL-PCL group (n=5), the defect was implanted with DL-PCL scaffold and for the SHAM group (n=5), the defect was left empty. The wound was closed with a 4-0 nylon suture. The DL-PCL scaffolds were prepared as a circular disk as described above in the culture section.

#### **Quantitative analysis of immunoglobulin G (IgG) with enzyme-linked immunosorbent assay (ELISA)**

Whole blood was collected via rat tail before performing the implantation (0 week), two, four and eight

weeks after implantation. The blood centrifugation is made with 10,000 rpm to separate the red blood cells. Then, quantitative detection of rat IgG was done using the Rat IgG ELISA Kit (abcam, MA, USA) with a spectrophotometer at 450 nm. Serum IgG was compared between the SHAM and the DL-PCL groups.

#### **Micro-Computed Tomography (Micro-CT)**

Bone formation in the calvarial defect at 4 and 8 weeks were analyzed using micro-CT imaging. After being euthanized using pentobarbital intraperitoneal injection, the calvarial bones were carefully excised, cleaned and fixed immediately with 10% (v/v) formaldehyde for 24 hours and kept in PBS. Then, the samples were assessed using 35 SCANCO MEDICAL Micro-CT (70 kVp, 114  $\mu$ A, 8 W with 15  $\mu$ m Voxel; SCANCO, Switzerland) for bone mineral density and bone morphology in the defect area. The analyses were performed using 3D analysis software from Scanco Medical (SCANCO Medical AG, Switzerland).

#### **Histological examination**

After micro-CT analysis, the specimens were dehydrated in graded ethanol solutions, embedded in paraffin, coronal sectioned (5  $\mu$ m in thickness), and stained with Masson's Trichrome to demonstrate osteon and cellular detail. The digital images of the sections were obtained by a visual slide microscope (Mirax desk, Carl Zeiss, Germany).

### **Statistical Analysis**

Statistical analysis was performed using the independent *t*-test for mineral density of micro-CT data. Differences at  $p < 0.05$  were considered statistically significant. All statistical analyses were performed using Statistical Package for the Social Science (SPSS) Statistics software package version 22 (IBM, New York, USA).

## Results

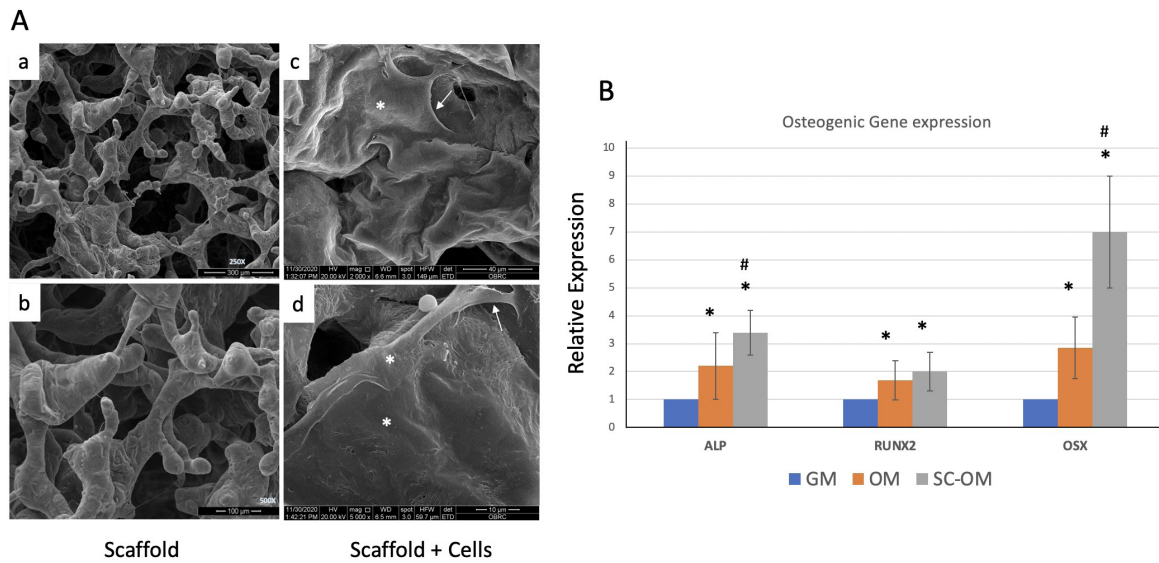


**Figure 1** (A) SEM images at 250x (a) and 500x (b) magnification illustrating the microstructures of the DL-PCL scaffold. Representative SEM images illustrating the morphology of PDL cells cultured for 16 hours on DL-PCL scaffolds (c and d with the magnification of 2000x and 5000x, respectively). Note the well spread cells (\*) on the surface of the scaffold. White arrow showed the border of cells that extended over the attached cells. (B) Graph showed the results from real-time RT-PCR analysis to examine the expression of osteogenic markers ALP, RUNX2, and OSX cultured for 2 days. In growth medium (GM) or osteogenic medium (OM) and in DL-PCL scaffold using OM medium (DL-PCL) \* indicated the significance when compared to GM, # indicated the significance when compared to OM at  $p < 0.5$

### Cell adhesion and differentiation

The biocompatibility of DL-PCL scaffold was evaluated in terms of its ability to support cell attachment and differentiation. Fig. 1(A) shows SEM images of DL-PCL with and without PDL cells. Cells were seeded onto the DL-PCL scaffolds for 16 hours and then processed by SEM analysis. The image of the DL-PCL 3D-scaffold showed good interconnected porosity and the appearance of a polymeric network (Fig.1A; a and b). The figure also showed well-spread PDL cells after 16 hours seeded on the scaffold. The majority of cells showed evidence of the extension and expansion over the area of the scaffolds.

### Comparison of osteogenic gene expression by RT-PCR analysis

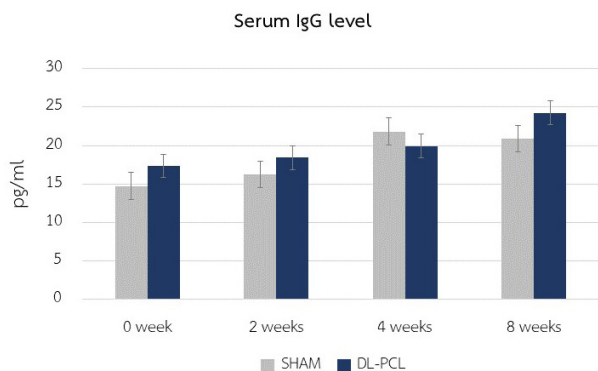
The osteogenic differentiation was monitored based on the expression of three key osteogenic related genes including ALP an early marker of osteogenic differentiation, RUNX2 and OSX, the key transcription factors that induced osteogenic differentiation. The results in

Fig.1B showed upregulation of ALP, RUNX2 and OSX mRNAs expression in cells cultured with OM medium for two days compared to the cells cultures in GM. The results also indicated that cell culture on the DL-PCL scaffold showed the increased expression of these three genes compared to those in the OM medium as analysed by real-time RT-PCR.

### Quantitative analysis of IgG levels in rat

The scaffold was implanted in the rat calvarial defect model. Fig. 2 showed the schematic of calvarial defects and the implant of the scaffold in the defects. The defects were created with 5 mm diameter trephine bur within the temporal bone. The defects were left empty (SHAM) or filled with the DL-PCL scaffold for up to 8 weeks. To evaluate the specific-immune response, the amount of total IgG from the serum was measured. The results did not show any significant differences between the level of serum IgG in both the SHAM and the DL-PCL groups at all time points (0-8 weeks).





**Figure 2** Graph showed the level of serum IgG of the rat in the SHAM and DL-PCL groups. No significant difference was detected

### **In vivo bone formation of DL-PCL scaffolds in rat calvarial model**

The amount of new bone formation in the defect was assessed by micro-CT analysis after four and eight

weeks of implantation. Quantification of bone volume/total volume (BV/TV) showed the amount of new bone formation at four and eight weeks of DL-PCL group was significantly higher than the SHAM group ( $P < 0.05$ ) [Fig. 3].

Histological analysis of specimens at four and eight weeks after implantation were shown in Fig. 4. At four weeks, the DL-PCL group was found to have an increase in the amount of collagen, osteoid formation and vascularization inside the scaffold. At eight weeks, woven bone structures, osteocytes and lacunae structures were prominent and the newly formed bone in the center of the defect was seen. In contrast, the defects in the SHAM group were filled with loose connective tissue and minimal mineralization at either time point.

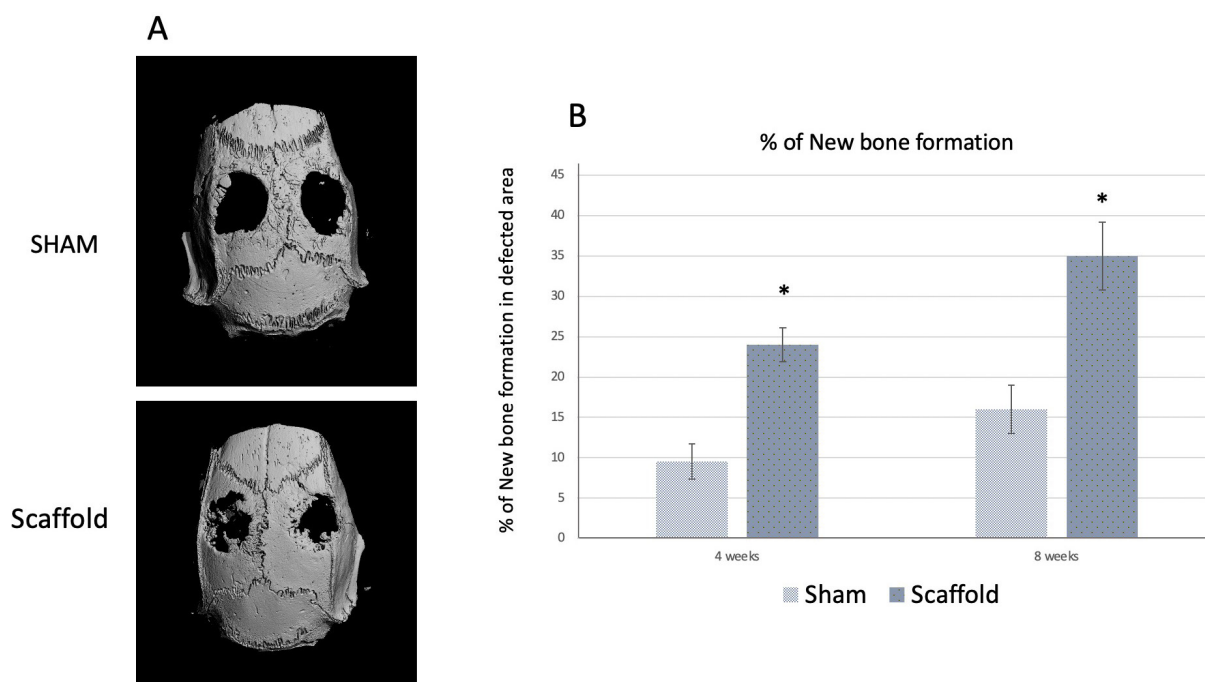


**Figure 3** (A) Picture from micro-CT analysis showed the amount of new bone formation compared between SHAM and DL-PCL groups after 4 and 8 weeks implantation. (B) Graph showed the quantitative amount of new bone formation as calculated by bone volume/total defect volume (BV/TV). \* indicated the significance when compared to SHAM at  $p < 0.5$

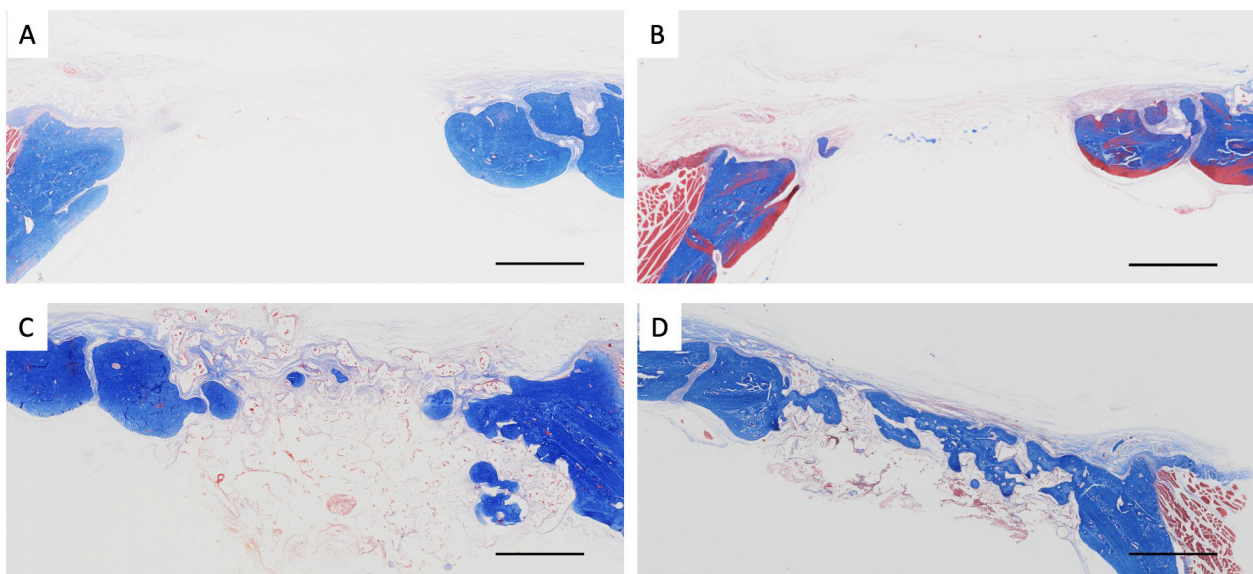


**Figure 4** Decalcified histological sections of rat calvarial at 4 and 8 weeks in the SHAM and the DL-PCL groups. a and b showed the section from SHAM after 4 and 8 weeks, respectively. Fibrous tissue was found in the center of the defect. New bone formation could be observed at the edge of the defect. c and d showed the section from the DL-PCL group at 4 and 8 weeks, respectively. New bone formation could be observed within the implanted scaffold. Black bars represented 1 mm

## Discussion

The data from this present study showed the ability of three-dimensional DL-PCL scaffold to support cell adhesion and differentiation both *in vitro* and *in vivo*. The use of PCL scaffold for bone tissue engineering had been report in several studies, however, the majority of bone grew outside the scaffold.<sup>15,16</sup> On the contrary, using our fabrication method, i.e., improve the connectivity between porous, can find the ossification centre that occurred within the scaffold, indicating the enhance ability of the scaffold to support the de novo bone formation.

In terms of cell adhesion, the SEM showed the well spreading of PDL cells on DL-PCL scaffold within 16 hours. The flatten of the cells on the surface of the scaffold indicated the good biocompatibility of the scaffold. This may be due to not only the high porosity and highly interconnected pore networks of the scaffold that allowed the cells to penetrate the scaffold<sup>17,18</sup> but also to the architecture of the scaffold that is similar to the fibrous network.

Not only supporting cell adhesion, cell culture on the DL-PCL scaffold could undergo osteogenic differentiation as judged by the increased expression of ALP, RUNX2 and OSX. ALP is the enzyme that provides to increase the local concentration of inorganic phosphate, a mineralization promoter, and to decrease the concentration of extracellular pyrophosphate, an inhibitor of mineral formation.<sup>19</sup> ALP has been considered to be one of the markers that represent the osteogenic differentiation.<sup>20</sup> RUNX2 and OSX are the key transcription factors that regulate osteogenic differentiation.<sup>21,22</sup> An increase of these two genes have been considered as cell undergoes osteogenic differentiation. The higher level of expression of ALP and OSX in cells cultured on the DL-PCL with the OM group compared to cells cultured with OM alone suggested the possibility that the DL-PCL architecture might help promote the cells differentiation. Similar to the present results, Chuenjitkuntaworn *et al.*<sup>23</sup>, reported the significant increase in the expression of type I collagen and osteocalcin mRNAs for the primary

human bone cells cultured on the PCL/HAp and the PCL scaffolds fabricated by combined solvent casting and particulate leaching techniques using sucrose as the porogen.

The ability to support bone cell adhesion and differentiation of DL-PCL scaffold is the key issue determining the success in new bone formation. In order to explore the potential of clinical applications, an *in vivo* study of the scaffold to repair a calvarial defect was performed. The interaction between the scaffold and specific-immune response was analyzed through the serum IgG of rats. Increased serum IgG level at four and eight weeks post-operatively from baseline was probably due to surgical trauma which lead to endogenous upregulation of IgG.<sup>24</sup> There was no significant difference when comparing the IgG levels the of SHAM and DL-PCL groups at all time points, suggesting that B-lymphocyte activity or adaptive immune response was in a range expected for the calvarial defect. Furthermore, an histological analysis saw no foreign body reaction around DL-PCL scaffolds. Thus, the DL-PCL scaffold may become the biocompatible option for tissue engineering. Similarly, Nisbet *et al.*<sup>25</sup> reported the extent of microglial and astrocytic responses following the implantation of an electrospun PCL scaffold on the rat brain. The inflammatory microglia peaked at around four days and persisted for 28 days. Astrocytes displayed a similar pattern of activation. However, 60 days after implantation, there were no scars or foreign body reactions detected surrounding the scaffolds.

Finally, bone regeneration in the calvarial defects of rats was assessed. During the operation, good retention of the DL-PCL scaffolds on the implant site was observed. This may be due to ample drainage of the exudate through the pore structure of the scaffold prevents the accumulation of exudate beneath the scaffold, which may dislodge the scaffold due to the pressure build-up.<sup>23</sup> From a histological view, new blood vessels with red blood cells were formed in the groups receiving DL-PCL scaffold implantation. This suggests the regeneration of vascularized bone tissue by the scaffold. Vascularization is critical for bone regeneration and persistence of newly formed bone tissue mass.<sup>26</sup>

Furthermore, micro-CT data demonstrated a significant increase in BV/TV in the defects of the DL-PCL group at four and eight weeks post-surgery and from histological analysis, the degradation of scaffold and the newly formed bone in the center of the defect in the DL-PCL group at eight weeks after implantation were identified. Interestingly, the appearance of new bone area both at the center and edge of the DL-PCL scaffold group made them significantly increased bone volume greater than the SHAM group and indicate the excellent osteoconductivity of the DL-PCL scaffolds, when implanted *in vivo*. This ability might come from the highly interconnected pore networks of the scaffolds to facilitate cells ingrowth<sup>10</sup> as well as the fibrous like structure of the scaffold.

Regarding the degradation rate of PCL, there was a report showing that the degradation time for the PCL scaffold ranged between 21 days to two years.<sup>16</sup> Generally, a scaffold was designed to allow the seeded cells to proliferate and secrete extracellular matrix, therefore the gradual degradation of the scaffold will provide space for new cell growth.<sup>10</sup> In addition, the water absorption ability of the DL-PCL scaffold may facilitate specific adsorption of serum proteins that could help regulate the adhesion and proliferation of the cells.<sup>23,27</sup> Consider the amount of scaffold left in the affected area between four and eight weeks; approximately half of the scaffold already had degraded. Therefore, the degradation of the scaffold should be within three to six months, which would be the reasonable time frame in craniomaxillofacial applications.<sup>28</sup>

In conclusion, this study suggests that the DL-PCL scaffold was suitable for bone defect repair in a critical size rat calvarial defect model. The novel DL-PCL scaffold could serve as a carrier for repairing bone defects. This scaffold has enormous potential to develop as material for bone tissue engineering applications. Further experimental and clinical studies should be conducted to confirm these results.

## Acknowledgement

This study was supported by the 2012 Research Chair Grant from the National Science and Technology



Development Agency (NSTDA). The Center of Excellence for Regenerative Dentistry was supported by the Chulalongkorn Academic Advancement into Its 2nd Century Project.

## References

1. Wan DC, Nacamuli RP, Longaker MT. Craniofacial bone tissue engineering. *Dental Clinics* 2006;50(2):175-190.
2. Ayoub A, Al-Fotawei R. Biomaterials in the reconstruction of the oral and maxillofacial region. *Front Oral Biol* 2015;17:101-14.
3. Liu Y, Lim J, Teoh SH. Development of clinically relevant scaffolds for vascularised bone tissue engineering. *Biotechnol Adv* 2013; 31(5):688-705.
4. Mobini S, Ayoub A. Bone tissue engineering in the maxillofacial region: The state-of-the-art practice and future prospects. *Regeneration, Reconstruction, & Restoration* 2016;1(1):8-14.
5. Wu S, Liu X, Yeung KW, Liu C, Yang X. Biomimetic porous scaffolds for bone tissue engineering. *Mater Sci Eng R* 2014;80:1-36.
6. Murphy CM, O'Brien FJ, Little DG, Schindeler A. Cell-scaffold interactions in the bone tissue engineering triad. *Eur Cell Mater* 2013;26:120-32.
7. O'Brien FJ. Biomaterials & scaffolds for tissue engineering. *Materials today* 2011;14(3):88-95.
8. Burg KJ, Porter S, Kellam JF. Biomaterial developments for bone tissue engineering. *Biomaterials* 2000;21(23):2347-2359.
9. De Witte T-M, Fratila-Apachitei LE, Zadpoor AA, Peppas NA. Bone tissue engineering via growth factor delivery: from scaffolds to complex matrices. *Regen Biomater* 2018;5(4):197-211.
10. Hutmacher DW. Scaffolds in tissue engineering bone and cartilage. In: *The Biomaterials: Silver Jubilee Compendium*. Elsevier; 2000: 175-189.
11. Salgado AJ, Coutinho OP, Reis RL. Bone tissue engineering: state of the art and future trends. *Macromol Biosci* 2004;4(8):743-765.
12. Marletta G, Ciapetti G, Satriano C, Perut F, Salerno M, Baldini N. Improved osteogenic differentiation of human marrow stromal cells cultured on ion-induced chemically structured poly-ε-caprolactone. *Biomaterials* 2007;28(6):1132-1140.
13. Sinha V, Bansal K, Kaushik R, Kumria R, Trehan A. Poly-ε-caprolactone microspheres and nanospheres: an overview. *Int J Pharm* 2004; 278(1):1-23.
14. Thadavirul N, Pavasant P, Supaphol P. Development of polycaprolactone porous scaffolds by combining solvent casting, particulate leaching, and polymer leaching techniques for bone tissue engineering. *J Biomed Mater Res A* 2014;102(10):3379-3392.
15. Williams JM, Adewunmi A, Schek RM, Flanagan CL, Krebsbach PH, Feinberg SE, *et al*. Bone tissue engineering using polycaprolactone scaffolds fabricated via selective laser sintering. *Biomaterials* 2005; 26(23):4817-4827.
16. Roosa SMM, Kempainen JM, Moffitt EN, Krebsbach PH, Hollister SJ. The pore size of polycaprolactone scaffolds has limited influence on bone regeneration in an *in vivo* model. *J Biomed Mater Res A* 2010;92(1):359-368.
17. Karageorgiou V, Kaplan D. Porosity of 3D biomaterial scaffolds and osteogenesis. *Biomaterials* 2005;26:5474-5491.
18. Takahashi Y, Tabata Y. Effect of the fiber diameter and porosity of non-woven PET fabrics on the osteogenic differentiation of mesenchymal stem cells. *Biomater Sci Polym* 2004;15:41-57.
19. Golub EE, Boesze-Battaglia K. The role of alkaline phosphatase in mineralization. *Current Opinion in Orthopaedics* 2007;18(5):444-448.
20. Endres M, Hutmacher DW, Salgado AJ, C Kaps, J Ringe, R L Reis, *et al*. Osteogenic Induction of Human Bone Marrow-Derived Mesenchymal Progenitor Cells in Novel Synthetic Polymer-Hydrogel Matrices. *Tissue Eng* 2003;9(4):689-702.
21. Liddo R, Paganin P, Lora S, Dalzoppo D, Giraudo C, Miotto D, *et al*. Poly-ε-caprolactone composite scaffolds for bone repair. *Int J Mol Med* 2014;34:1537-1546.
22. Sinha KM, Zhou X. Genetic and molecular control of osterix in skeletal formation. *J Cell Biochem* 2013;114(5):975-84.
23. Chuenjitkuntaworn B, Inrung W, Damrongsri D, Mekaapiruk K, Supaphol P, Pavasant P. Polycaprolactone/hydroxyapatite composite scaffolds: preparation, characterization, and *in vitro* and *in vivo* biological responses of human primary bone cells. *J Biomed Mater Res A* 2010;94(1):241-251.
24. Fishman JM, Wiles K, KJ W. CHAPTER 8 - The Acquired Immune System Response to Biomaterials, Including Both Naturally Occurring and Synthetic Biomaterials. *Host Response to Biomaterials* 2015: 151-187.
25. Nisbet DR, Rodda AE, Horne MK, Forsythe JS, DI F. Neurite infiltration and cellular response to electrospun polycaprolactone scaffolds implanted into the brain. *Biomaterials* 2009:4573-4580.
26. Santos M, Reis R. Vascularization in Bone Tissue Engineering: Physiology, Current Strategies, Major Hurdles and Future Challenges. *Macromol Biosci* 2010;10:12-27.
27. Hariraksapitak P, Suwantong O, Pavasant P, Supaphol P. Effectual drug-releasing porous scaffolds from 1,6-diisocyanatohexane extended poly(1,4-butylene succinate) for bone tissue regeneration. *Polymer Elsevier* 2008;49:2678-2685.
28. Bose S, Roy M, Bandyopadhyay AJTib. Recent advances in bone tissue engineering scaffolds. *Trends Biotechnol* 2012;30(10):546-554.